Molecular basis for recognition of the Group A Carbohydrate backbone by the PlyC streptococcal bacteriophage endolysin

Harley King[1,^], Sowmya Ajay Castro[2,^], Juan A. Bueren-Calabuig[3,^], Amol Arunrao Pohane[4], Cynthia M. Scholte[1], Vincent A. Fischetti[5], Natalia Korotkova[4,6] ,Fabio Zuccotto[3], Daniel C. Nelson[1] and Helge C. Dorfmueller[2,*]

[1]Institute for Bioscience and Biotechnology Research, University of Maryland, Rockville, MD, USA

[2]Division of Molecular Microbiology, School of Life Sciences, University of Dundee, Dundee, UK

[3]Drug Discovery Unit, Wellcome Centre for Anti-Infectives Research, Division of Biological Chemistry, School of Life Sciences, University of Dundee, Dundee, UK

[4]Department of Microbiology, Immunology and Molecular Genetics, University of Kentucky, Lexington, Kentucky, USA

[5]Laboratory of Bacterial Pathogenesis and Immunology, The Rockefeller University, New York, NY, USA

[6]Department of Molecular and Cellular Biochemistry, University of Kentucky, Lexington, KY, USA

[^]equal contribution

[*]Correspondence: Helge C. Dorfmueller, h.c.z.dorfmueller@dundee.ac.uk

Keywords: Streptococcus; rhamnose, polysaccharide, cell wall, bacteriophage, endolysin, pyogenes

27 **Abbreviations (alphabetical order)**

28 Cell wall-binding domain (CBD), enzymatically active domain (EAD), Glucose (Glc), glycerol
29 phosphate (GroP), Glycosyl Hydrolase (GlyH), Group A Carbohydrate (GAC), Group A
30 Streptococcus (GAS), Group A-variant Streptococcus (GAVS), Group C Carbohydrate (GCC),
31 Group C Streptococcus (GCS), Group G Carbohydrate (GGC), *N*-acetyl-glucosamine (GlcNAc),
32 *N*-acetyl-galactosamine (GalNAc), N-acetyl-muramic acid (MurNAc), Peptidoglycan (PG),
33 polyrhamnose (pRha), Rhamnose (Rha), *S. dysgalactiae subsp. equisimilis* (SDSE), *S. mutans*
34 serotype c carbohydrate (SCC)

35

36

Abstract

Endolysins are peptidoglycan (PG) hydrolases that function as part of the bacteriophage (phage) lytic system to release progeny phage at the end of a replication cycle. Notably, endolysins alone can produce lysis without phage infection, which offers an attractive alternative to traditional antibiotics. Endolysins from phage that infect Gram-positive bacterial hosts contain at least one enzymatically active domain (EAD) responsible for hydrolysis of PG bonds and a cell wall binding domain (CBD) that binds a cell wall epitope, such as a surface carbohydrate, providing some degree of specificity for the endolysin. Whilst the EADs typically cluster into conserved mechanistic classes with well-defined active sites, relatively little is known about the nature of the CBDs and only a few binding epitopes for CBDs have been elucidated. The major cell wall components of many streptococci are the polysaccharides that contain the polyrhamnose (pRha) backbone modified with species-specific and serotype-specific glycosyl side chains. In this report, using molecular genetics, microscopy, flow cytometry and lytic activity assays, we demonstrate the interaction of PlyCB, the CBD subunit of the streptococcal PlyC endolysin, with the pRha backbone of the cell wall polysaccharides, Group A Carbohydrate (GAC) and serotype *c*-specific carbohydrate (SCC) expressed by the Group A Streptococcus and *Streptococcus mutans*, respectively. Molecular dynamics simulations reveal a previously unidentified binding pocket that is regulated by a gatekeeper residue and uncover that a previously reported inactive PlyC mutant is locked into a ‘closed’ conformation. Docking studies with the short GAC backbone oligosaccharides expose potential protein-carbohydrate interactions and are consistent with PlyCB binding to the unmodified pRha or pRha decorated with the GAC side chains.

61 **Introduction**

62 Endolysins are bacteriophage-encoded PG hydrolases that normally function from within the cell
63 to lyse the bacterial host, releasing progeny phage and completing the phage lifecycle [1].
64 However, the lytic activity of endolysins can be harnessed for antimicrobial use due to their
65 ability to equally lyse bacteria when applied exogenously, without infection by a parental phage.
66 Due to their direct lytic action on target PG, endolysins are not affected by efflux pumps,
67 alterations in metabolism, or other mechanisms of antibiotic resistance, making them ideal
68 candidates for development against multi-drug resistant organisms [2-4]. Notably, at least three
69 endolysins, some of which are active against methicillin-resistant *Staphylococcus aureus*, are
70 currently being evaluated in human clinical trials for their antimicrobial activity (reviewed in [5]).
71
72 Most endolysins, and in particular those from phage that infect Gram-positive bacterial hosts,
73 are comprised of modular domains. An enzymatically active domain (EAD) is generally found in
74 the N-terminal region, while a cell wall-binding domain (CBD) is located in the C-terminal region
75 [6]. As the name implies, the EAD is a catalytic domain that is responsible for cleaving specific
76 bonds in the PG, the nature of which is dependent on the mechanistic class of the EAD.
77 Occasionally, endolysins contain two EADs, although both are not necessarily active. The CBD
78 binds at high affinity [7] to a cell wall-specific epitope and was suggested to dictate genus,
79 species and serovar-specificity of the endolysin. The CBD targets may be surface
80 carbohydrates, wall teichoic acids linked to the Gram-positive bacterial cell wall, or the PG itself
81 [8].
82
83 The endolysin now known as PlyC is one of the first described endolysins and remains one of
84 the most studied. In 1934, Alice Evans noted a “nascent lysis” activity derived from
85 streptococcal phage lysates on streptococcal strains that were not sensitive to the phage itself
86 [9]. By 1957, Krause had determined that the phage used by Evans was specific for Group C

87 Streptococci (GCS), but an “enzyme” produced by the phage could lyse Groups A, A-variant,
88 and C Streptococci (GAS, GAVS, and GCS, respectively) [10]. These findings were confirmed
89 by Maxted later the same year and extended to include Group E Streptococci (GES) [11]. In
90 2001, PlyC, then referred to as the streptococcal C_1 lysin, became the first endolysin to be used
91 therapeutically, protecting mice from GAS challenge in a nasopharyngeal model [2].
92 Subsequent studies revealed that PlyC is a structurally unconventional endolysin, which is not
93 encoded by a single gene as found for all other endolysins described to date. Rather, PlyC is a
94 nine-subunit holoenzyme encoded by two distinct genes, *plyCB* and *plyCA*, within a
95 polycistronic operon [12]. Eight PlyCB subunits self-assemble into a ring structure and form the
96 basis of the CBD that binds the streptococcal surface. A single PlyCA subunit contains two
97 distinct EADs separated by an extended α-helical linker region, which interfaces with the N-
98 terminal residues of the PlyCB octamer [13]. The PlyCA EADs consist of a glycosyl hydrolase
99 (GH) domain and a cysteine, histidine-dependent aminohydrolase/peptidase (CHAP) domain.
100 The very high lytic activity of PlyC relative to other endolysins is attributed to
101 synergy/cooperativity between the two EADs.
102
103 Although the EADs of PlyCA have been extensively characterized with respect to specificity of
104 PG bonds they cleave, active-site residues, and their synergistic activity, it is unclear how PlyCB
105 recognizes PG of GAS, GCS and GES. Similar to other Gram-positive bacteria, the plasma
106 membrane of streptococci is surrounded by thick cell wall that consists of a complex network of
107 PG with covalently attached polysaccharides. Rebecca Lancefield utilized the unique
108 immunogenicity of the surface carbohydrates in β-hemolytic streptococci to subsequently
109 separate them into serogroups [14]. *S. pyogenes* is categorized as Group A Streptococcus,
110 whilst *S. dysgalactiae subsp equisimilis* (SDSE) produce at least two types of carbohydrates
111 and are annotated as Group C and G Streptococci, respectively [15]. Pioneering work by many
112 researchers have revealed that the cell wall polysaccharides of GAS, GCS and *S. mutans*,

113 consist of a pRha backbone modified with species-specific and serotype-specific glycosyl side
114 chains (Fig. 1A) [16, 17]. In GAS, GCS and *S. mutans* serotype *c*, the polysaccharides termed
115 the Lancefield group A carbohydrate (GAC), group C carbohydrate (GCC), and SCC,
116 respectively, have a conserved repeating →3)α-Rha(1→2)α-Rha(1→ di-saccharide backbone
117 [16, 17]. The β-*N*-acetylglucosamine (GlcNAc) side chains are attached to the 3-position of the
118 α-1,2 linked rhamnose (Rha) in GAC [16, 18, 19]. The GCC side chains have two *N*-acetyl-
119 galactosamine (GalNAc) residues attached to the same hydroxyl of Rha [16, 18, 20]. SCC
120 carries the α-glucose (Glc) side chains attached to the 2-position of the α-1,3 linked Rha in SCC
121 [17]. Additionally, the side chains of GAC and SCC are decorated in parts with the glycerol
122 phosphate (GroP) moiety [21]. The GAC and SCC biosynthetic pathways are encoded by the
123 12-gene loci *gacABCDEFGHIJKL* and *sccABCDEFGHMNPQ*, respectively. The molecular
124 mechanisms of GAC and SCC biosynthesis have been the focus in a number of recent studies
125 [21-25].
126
127 Remarkably, extracted GAC is known to partially inhibit the lytic actions of PlyC [26].
128 Furthermore, a GAS mutant carrying the unmodified GAC (lacking the GlcNAc side chains)
129 displayed enhanced susceptibility to PlyC [25], implicating PlyCB in recognition of the pRha
130 backbone. Here, we identify the pRha backbone of GAC as the definite minimal binding epitope
131 for PlyCB. Molecular dynamics simulations and docking studies based on our findings further
132 establish a model of interaction between PlyCB and selective surface carbohydrates in
133 streptococci.
134
135 **Materials and Methods**
136 **Bacterial strains, growth conditions and media**
137 *Streptococcus pyogenes* strain D471 was propagated on solid media in plates containing Todd-
138 Hewitt broth supplemented with yeast extract (0.2%) (THY) and agar (1.4%) or in liquid THY as

139 described by Gera et al [27]. *S. mutans* wild type (Xc) and mutants were grown in Todd-Hewitt
140 broth with 1% yeast extract. All cultures were grown without antibiotics and without aeration at
141 37°C. *E. coli* genotypes DH5α (NEB, cat. No. C2988J), DH10α (Thermo Fisher, cat No.
142 18297010), BL21 (NEB, cat No. C2530H) and Origami 2 (Millipore Sigma, cat. No. 71346) were
143 used for routine plasmid propagation or protein expression and grown in Lysogeny Broth (LB)
144 medium supplemented with either 50 µg/ml kanamycin, 100 µg/ml ampicillin or 35 µg/ml
145 chloramphenicol as needed.
146
147 Bacterial strains *E. coli* CS2775 were transformed with pRGP1 plasmid [28], *gacABCDEFG* [23]
148 to produce pRha or empty plasmid control (pHD0131). The bacterial cells were grown overnight
149 in LB containing erythromycin (150 µg/ml) at 37°C and used next day for whole cell Western
150 blots and FACS and microscopy analysis.
151
152 **Recombinant expression and purification of PlyCB$_{WT}$ and PlyCB$_{R66E}$**
153 PlyCB$_{WT}$ (GenBank ID: NC_004814.1:7517-7735) was expressed from a pBAD24 vector and
154 purified from BL21 cells as previously described [12]. In brief, the culture was grown in LB and
155 induced with 0.25% L-arabinose at OD_{600} ~1.2-1.4 (Alfa Aesar, cat no. A11921). Cultures were
156 grown at 37°C with shaking at 180 RPM for 3-4 hours, centrifuged at 4500 x g and resuspended
157 in phosphate-buffered saline (PBS). Lysis was performed by a French press (1800 psi).
158 Benzonase (Millipore Sigma, cat. No. 70746-3) was added and the lysate incubated at room
159 temperature with rotation for 20-30 min. The lysate was centrifuged at 20,000 x g for 20 min and
160 the cleared lysate was passed through a 0.45-µm filter and loaded onto a XK-26/20 column
161 (Cytiva) with 30-35 ml ceramic hydroxyapatite (Bio-Rad, cat no. 1582000). PlyCB$_{WT}$ was eluted
162 from the column with three column volumes of 1 M sodium phosphate buffer (pH 7.2). Protein
163 was subsequently dialyzed in PBS, 10% glycerol and stored at -80°C until use. Protein
164 purification of PlyCB$_{R66E}$ was performed as PlyCB$_{WT}$ [13]. The fluorescent labeling of PlyCB$_{WT}$

165 and $PlyCB_{R66E}$ was performed using the manufacturer's recommended guidelines (Thermo
166 Fisher, cat. No. A20174).
167
168 **Purification of GAC**
169 GAS were grown overnight in THY media at 37˚C. Cultures were centrifuged at 4,500 x g.
170 Pellets were washed and resuspended in 40 ml distilled water per each original liter of media
171 used and combined in an 800 ml beaker. 22.5 ml 4N sodium nitrite (5 ml per liter of culture) was
172 added to the beaker in addition to 22.5 ml glacial acetic acid (5 ml per liter of culture). An orbital
173 shaker was used to gently mix the beaker for 15 min in a hood. The mixture was centrifuged in
174 500 ml bottles at 8000 x g for 15 min. The supernatant was decanted to a new beaker and
175 neutralized with 1M sodium hydroxide. The total solution, about 300 ml, was filtered with a 0.45-
176 micron filter assembly. 50-50 ml aliquots were deposited in a 3.5 kDa membrane and dialyzed in
177 a 4-liter beaker overnight with water. The following day, the solution was concentrated using an
178 Amicon 400 ml stirred cell (model 8400) filter assembly with a 76 mm diameter Ultracel® 5 kDa
179 ultrafiltration disc (Millipore Sigma, cat. No. PLCC07610) for 2 hours with 60 psi. The ~10 ml
180 concentrate was loaded onto an S-100 column for final purification. Fractions were assayed for
181 Rha, lyophilized and stored at 4°C until use.
182
183 **Calculation of pRha concentration**
184 A modified protocol by Edgar *et al.* [21] based on a protocol from DuBois *et al.* [29] was used to
185 determine Rha concentration in purified GAC. Briefly, anthrone reagent was prepared by
186 dissolving 0.2% w/w anthrone in H_2SO_4. Eighty microliters of aqueous samples or standards
187 containing either GAC or L-Rha at known concentrations were added to a 1.5 ml microfuge
188 tube. To this same tube, 320 µL of the anthrone reagent was added. Samples were boiled at
189 98°C for 10 min in a heat block. Samples were cooled to room temperature, transferred to a

190 quartz plate, and the absorbance at 580 nm was recorded using a spectrophotometer. Rha
191 concentration was interpolated using an L-Rha standard curve.
192
193 **Precipitation of PlyCB with GAC**
194 $PlyCB_{WT}$ and $PlyCB_{R66E}$ samples were defrosted from storage at -80°C. Lyophilized GAC was
195 resuspended in PBS. Both proteins and GAC were added to a 3.5 kDa dialysis membrane and
196 dialyzed overnight in PBS. Protein concentrations were determined using a NanoDrop
197 spectrophotometer (Thermo Fisher ND-2000) at 280 nm and were diluted to 5 mg/ml. The GAC
198 was also assayed and diluted with PBS to 1.6 mg/ml. One-hundred microliters of proteins and
199 100 µl of GAC or PBS were mixed in a 250 µl quartz plate and allowed to incubate without
200 shaking at room temperature. Visible precipitate formed in samples in 5-8 minutes. After
201 recording the precipitate at 340 nm using a Spectramax® M5 (Molecular Devices)
202 spectrophotometer, the total sample volume was transferred to a 1.5 ml microfuge tube.
203 Samples were centrifuged at 14,000 x g to pellet the precipitate and supernatants were
204 transferred to new 1.5 ml microfuge tubes. Two-hundred microliters of 8M urea was added to
205 the pellet. Pellets were resuspended and 5 µl of either pellet or supernatant were added to 40 µl
206 water with 8 µl 6x Laemmli buffer with DTT. Samples were boiled at 98°C for 8 min, and then
207 12.5 µl were loaded onto a 7.5% SDS-PAGE and run for 32 min at 200V. Proteins were
208 visualized using Coomassie stain.
209
210 **Lysis assay**
211 A turbidity reduction assay was used to ascertain strain sensitivity to PlyC. This assay was
212 performed as previously described [30], except PlyC was used at 2 µM. Eight technical
213 replicates were performed.
214

215 Sensitivity of streptococcal species to PlyC-mediated lysis was analyzed using a wide range of
216 clinical isolates: 1) GAS isolates: $M1_{UK}$, WT 5448 strain [M1], delta*gacI* 5448 strain [d*gacI*]; 2)
217 GCS isolate: stC74A.0; 3) SDSE_*gac* isolates: stG245.0, stG652.0. stG485.0; GGS: stG6.0,
218 stG485.0 and 4) *S. mutans* serotype c were used as negative controls. Briefly, all streptococcal
219 strains were grown in THY at 37˚C overnight in 5% CO_2, except for *S. mutans*, which was grown
220 in THB media. Next day, the bacterial cells were inoculated in 1:100 fresh media and grown until
221 mid-logarithmic phase (OD_{600} 1.0). The cells were washed in PBS and resuspended to an OD_{600}
222 of 2.0. In a 96-well plate, to a 100 µl of bacterial cells, 100 µl of PlyC [1 µg/ml] was added and
223 immediately read at an absorbance of OD_{600}. The obtained values were standardized by
224 subtracting from the background values. The data is plotted using GraphPad Prism version 9.
225

226 **SDS-PAGE and blotting analysis**

227 $PlyCB_{WT}$ binding to recombinant *E. coli* expressing pRha was conducted using blot analysis.
228 Briefly, the lysate from the overnight cultures was analyzed in 20% tricine gels. SDS-PAGE and
229 protein transfers were performed according to manufactures instructions, Atto Ae-6050 Mini Gel
230 chamber and Novex protein separation from Thermo Fisher, respectively. The PVDF
231 membranes were blocked with 5% non-fat dry milk with Tris-Buffered Saline, 0.1% Tween® 20
232 detergent prior to incubation with $PlyCB_{WT}$ labelled with Alexa Fluor® 647 (1:1000) for one hour
233 at room temperature. Goat anti-rabbit GAC antibodies conjugated with IRDye® 800CW were
234 used as a positive control (abcam ab216773). The resulting blots were imaged using the Licor
235 Odyssey FC Imaging System. All the blots were processed in parallel under the same
236 conditions.
237

238 **Microscopy**

239 Microscopic analysis of *E. coli* bacteria was performed using cells that were grown overnight in
240 LB supplemented with antibiotics at 37˚C and diluted 1:100 the next day and regrown until

241 OD_{600} reached 0.5. The cells were washed twice with PBS for 5 min at 10,000 rpm and stained
242 with 1:1000 dilution of $PlyCB^{AF647}$ and left for 20 minutes on ice in the darkness. Prior to fixing
243 the cells with 4% paraformaldehyde, the cells were washed again with PBS. The fixed cells
244 were mounted on 1% agarose coated microscopic slides and viewed under the CY5 channel on
245 a fluorescent Deltavision widefield microscope.
246
247 **FACS analysis**
248 *E. coli* cells were grown overnight as described above and diluted 1:100 the next day, grown at
249 37˚C and used for the assay at OD_{600} = 0.5. The cells were washed with PBS and probed with
250 $PlyCB^{AF647}$ or $PlyCB_{R66E}{}^{AF645}$ at 1:1000 dilution at 1:1000 dilution. Anti-GAC antibodies
251 conjugated with FITC (ABIN238144, antibodies-online, titer 1:50) were used as a positive
252 control. The samples were incubated for 20 minutes on ice at dark conditions. The cells were
253 washed twice with PBS at 14,000 rpm for 5 minutes and fixed with 4% paraformaldehyde. BD
254 LSRFortessa Flow Cytometry software was used to analyse the samples and the data
255 interpretation was conducted with FlowJo™ software v10.6.2.
256
257 **PlyC hydrolysis of sacculi**
258 *S. mutans* wild-type (WT) and the mutant strain sacculi were obtained by the SDS-boiling
259 procedure [25] followed by four washes each with 1 M NaCl and distilled water. The sacculi
260 were resuspended in PBS to OD_{600} of 1.0 and incubated with PlyC (5 µg/ml) in a 96-well plate.
261 The lysis was monitored after 10, 20, 30, 40, 50 and 60 min as a decrease in OD_{600}. Results
262 were reported as fold change in OD_{600} of the sacculi incubated with PlyC vs the sacculi
263 incubated without PlyC.
264
265 **Molecular Dynamics**

266 Monomers of $PlyCB_{WT}$ (PDB 4F87) and the $PlyCB_{R66E}$ mutant (PDB 4ZRZ) were simulated by
267 Molecular Dynamics (MD). The systems for MD simulations were prepared with the utility LEaP,
268 which is integrated in the suite of programs AMBER 16 [31]. The ff14SB force field [32] was
269 used. The N- and C-termini of the proteins were capped with an acetyl (ACE) and methylated
270 amino group (NME), respectively. Each simulated system was immersed in a water box (TIP3P
271 water model) and neutralized by adding the appropriate number of counterions. This was
272 followed by steepest-descent energy minimization to remove steric clashes. MD simulations
273 were performed using the pmemd.cuda module of AMBER 16. The cut-off distance for the non-
274 bonded interactions was set to 10Å. The periodic boundary conditions were used. Electrostatic
275 interactions were treated using the smooth particle mesh Ewald method [33]. The SHAKE
276 algorithm was applied to all bonds involving hydrogen atoms, and a time step of 2 fs was used
277 throughout [34]. Each energy minimized system was heated to 300K, equilibrated for 10 ns, and
278 further simulated for 2 μs without any restraints. Protein structures and MD trajectories were
279 visually inspected and analyzed using the molecular visualization programs PyMOL [35] and
280 VMD [36].
281
282 **Binding cavity identification and druggability assessment**
283 The site recognition software SiteMap, implemented in the Schrodinger suite of programs [37],
284 was used to investigate the cavities on the PlyCB wild type (PDB 4F87) and R66E mutant (PDB
285 4ZRZ) proteins surface, in terms of physicochemical properties (hydrophobic/hydrophilic
286 nature), volume, exposure, and enclosure. Based on those properties, an overall “SiteScore”
287 was generated providing an estimate value of the druggability of the pocket. Using the default
288 settings, scores of >= 0.8 define the limit between drug-binding and non-drug-binding cavities.
289
290 **Molecular docking**

291 A low energy 3D conformation of Rha di- and tri-saccharides was generated using LigPrep in
292 the Schrödinger platform [37]. The binding of the ligands in the Y28 gated cavity identified by
293 MD in the wild-type structure was evaluated by molecular docking. The program Glide [37], part
294 of the Schrodinger platform, was used in extra-precision mode with post-docking minimization.
295 No distance or hydrogen-bond constraints were applied. A 20Å cubic box centered on the
296 centroid of the residues Leu9, Phe10, His11, Thr12, Ser17, Tyr20 and Ile34 was used to
297 generate the docking grid. The default settings were modified to increase the conformational
298 sampling of rings by increasing the energy window to 6.0 kcal/mol.
299

300 **Results & Discussion**
301

302 **Pathogenic streptococci producing the GAC are susceptible to PlyC**

303 A major component of the GAS cell wall is the GAC, building approximately 50% of the cell wall
304 by weight [38]. The GAC is universally conserved amongst all isolated GAS strains on the basis
305 of the gene cluster sequence conservation [39]. A number of *S. dysgalactiae subsp. equisimilis*
306 (SDSE) isolates, naturally belonging to Group G Streptococci (GGS), have been reported to
307 have undergone homologous recombination and replaced their Group G Carbohydrate (GGC)
308 gene cluster in parts with the GAC gene cluster [40-42]. We therefore expanded the previously
309 reported PlyC streptococci cell lysis assay used by Nelson *et al.* [2] to investigate those new
310 isolates named SDSE_*gac*. We also tested if PlyC was able to lyse a selection of GAS
311 serotypes including a newly emerged isolate $M1_{UK}$ [43], and included negative controls GGS
312 isolates and *S. mutans* serotype C (Fig. 1B). In agreement with the published literature, all
313 tested GAS serotypes are susceptible to PlyC lysis and the two GGS isolates are resistant to
314 PlyC. The GGC does not contain the GAC, GCC and SCC pRha backbone with →3)α-
315 Rha(1→2)α-Rha(1→ di-saccharide repeats, but an alternating Rha-GalNAc carbohydrate [44]
316 (Fig. 1A). All three SDSE_*gac* isolates tested have inherited parts of the *gac* gene cluster and

317 produce the GAC instead of the GGC [41]. Strikingly, the SDSE_*gac* strains are all sensitive to
318 PlyC treatment. The fact that PlyC is able to lyse SDSE_*gac* strains that express the GAC, but
319 PlyC does not lyse the isogenic GGS strains producing the GGC strongly suggests that the
320 GAC is a critical component of PlyC recognition and subsequent activity.
321
322 Importantly, all strains tested in this study that are susceptible to PlyC lysis produce a cell wall
323 polysaccharide that contains the pRha backbone and a β-linked sugar substituent on the α1,2-
324 linked Rha (Fig 1A). We therefore suggest that the pRha backbone with and without a side
325 chain are both vital ligands to assist PlyC activity and the new SDSE_*gac* isolates will also be
326 susceptible to PlyC treatment due to production of the GAC.
327
328 **Purified GAC precipitates PlyCB - but not PlyCB$_{R66E}$**
329 The lysis assay of GAS cells, and in particular of the SDSE_*gac* variants, suggests that either
330 the ubiquitous pRha or GAC in GAS cells is the ligand for PlyCB. We propose that the PlyCB
331 octameric CBD binds GAC and/or the GAC pRha backbone. We tested this hypothesis by
332 investigating the binding of PlyC to partially purified GAC. We hypothesized if the GAC was able
333 to precipitate PlyCB, an interaction of the two systems must have occurred [45]. As a negative
334 control, we employed the previously published inactive mutant PlyCB$_{R66E}$, which lost the ability
335 to bind to GAS cells [13]. The purified proteins were incubated with the extracted GAC, and
336 precipitation was monitored at 340 nm, a standard wavelength for measuring protein
337 aggregation [46, 47] (Fig. 2A, B). Whilst keeping the PlyCB concentration constant, we varied
338 the concentration of GAC. Within five minutes at room temperature the solution became turbid,
339 suggesting aggregation (Fig. 2A). When the PlyCB concentration was kept constant and the
340 GAC concentration was varied, the turbidity correlated with PlyCB concentration in a dose
341 dependent manner, suggesting that PlyCB requires GAC to aggregate. Importantly, PlyCB did
342 not self-aggregate when no GAC was added in the assay. Furthermore, no aggregation was

343 detected when $PlyCB_{R66E}$ was incubated with purified GAC (Fig. 2B). To demonstrate the
344 presence of PlyCB in the precipitates, we analyzed the soluble and pellet fractions (Fig. 2C, D).
345 A higher yield of aggregated PlyCB was found in the pelleted samples when compared to the
346 soluble fraction (Fig. 2D). A similar precipitation effect was observed when we varied the PlyCB
347 concentration and kept the GAC concentration constant (Fig. 2E, F), demonstrating that both
348 species are necessary for an interaction.
349
350 When the L-Rha monosaccharide was mixed with PlyCB, no precipitation was observed,
351 suggesting that the GAC, or a moiety within the GAC, is a specific ligand required for PlyCB
352 precipitation.
353
354 **PlyCB binds to recombinantly produced pRha backbone**
355 The purified GAC from bacteria contains a mixture of carbohydrates, including the fully
356 decorated GAC with GroP[21] and a small proportion of the polysaccharide lacking the side
357 chains [48]. PlyC is able to lyse a number of GAS mutants including GAVS and d*gacI*_M1 [2,
358 11, 25, 49], that decorate the cell wall with the unmodified GAC lacking the side chains (Fig. 1A,
359 B), suggesting that the pRha backbone of the GAC is the minimal carbohydrate structure
360 required for PlyCB binding. To test this hypothesis, we recombinantly produced the pRha
361 backbone in *E. coli* cells. We and others have previously reported that the *S. mutans*
362 *sccABCDEFG* gene cluster, when transformed into *E. coli* cells, functionally produces the pRha
363 backbone attached to the lipid A [23, 28]. Additionally, to understand if PlyCB recognizes a
364 specific pRha backbone, we engineered *E. coli* cells expressing the GAC gene cluster
365 *gacABCDEFG* required for the GAC pRha production. *E. coli* cells carrying an empty plasmid
366 were used as a negative control.
367

368 Next, we investigated the binding of PlyCB conjugated with Alexa Fluor® 647 ($PlyCB^{AF647}$) to an
369 *E. coli* total cell lysate expressing the pRha backbone of the SCC or GAC, respectively (Fig.
370 3A). The blotted membranes were incubated with $PlyCB^{AF647}$, and a positive interaction between
371 $PlyCB^{AF647}$ and the *E. coli* produced pRha is visualized as a prominent band around 40 kDa.
372 The size of the band agrees with the band detected by anti-GAC antibodies that were previously
373 reported to recognize pRha [23] (Fig. 3B). Importantly, $PlyCB^{AF647}$ and GAC antibodies do not
374 interact with the cell lysate of *E. coli* expressing an empty plasmid (Fig. 3 A, B). We further
375 confirmed the ability of PlyCB to bind to *E. coli* cells decorated with the pRha by fluorescent
376 microscopy (S. F1). Only cells that produce the pRha are detected by the $PlyCB^{AF647}$, in
377 agreement with the results of the blot analysis.
378
379 To gather additional evidence that PlyCB interacts with the pRha backbone, we established a
380 flow cytometry assay to analyse the binding of $PlyCB^{AF647}$ to pRha-producing *E. coli*. Unstained
381 *E. coli* cells that express pRha or carry an empty plasmid sort in the identical range (Fig. 4A).
382 The GAC antibodies label exclusively the cells producing pRha (Fig. 4A). A similar pattern of the
383 GAC antibodies binding is observed when the cells were incubated with $PlyCB^{AF647}$ (Fig. 4B).
384 Contrary, the $PlyCB_{R66E}{}^{AF645}$ mutant protein does not bind to *E. coli* cells, and $PlyCB^{AF647}$ does
385 not interact with the cells expressing an empty vector (Fig. 4B). Taken together, these data
386 provide the first definitive evidence that the pRha backbone of GAC and SCC is a binding
387 receptor of the PlyCB octameric subunit.
388
389 **PlyC lyses engineered *S. mutans* producing the GAC**
390 Despite the fact that the SCC pRha backbone is identical to the GAC, *S. mutans* is resistant to
391 PlyC lysis (Fig. 1A). To get a better understanding why *S. mutans* is resistant to PlyC, we
392 compared PlyC-induced lysis of the sacculi purified from *S. mutans* WT and a number of mutant
393 strains producing different SCC variants (Fig. 5). First, we examined the Δ*sccH* mutant

394 producing the GroP-deficient SCC [21]. Similar to *S. mutans* WT, Δ*sccH* was resistant to PlyC-
395 mediated lysis (Fig. 5). Second, we tested the *sccN* deletion mutant, Δ*sccN*, that is deficient in
396 the enzyme required for generation of the Glc side chains [50]. A time dependent lysis is
397 observed for Δ*sccN*. Expression of the WT copy of *sccN* in Δ*sccN* (the Δ*sccN*:p*sccN* strain) fully
398 restored the resistance of the bacteria to PlyC (Fig. 5). These observations clearly suggest that
399 PlyC is able to bind to the *S. mutans* cells producing the unmodified pRha backbone, and the
400 Glc side chains in SCC hinders PlyC binding. We then investigated whether the addition of the
401 GAC GlcNAc side chains to the pRha backbone affects sensitivity of the engineered *S. mutans*
402 sacculi to PlyC-induced lysis. We expressed the GAS genes *gacHIJKL* required for the
403 formation and addition of the GlcNAc side chains and GroP to GAC [21], in the Δ*sccN*
404 background strain in two versions, creating the Δ*sccN:pgacHI*JKL* and Δ*sccN:pgacHIJKL*
405 strains [50]. The plasmid *pgacHI*JKL* contains an inserted stop codon in the *gacI* gene required
406 for generation of the GlcNAc side chain, and, therefore, the Δ*sccN:pgacHI*JKL* strain produces
407 the unmodified SCC lacking any side chains (Fig. 5). As expected, the sacculi isolated from this
408 strain remains susceptible to PlyC lysis. We previously showed that in Δ*sccN:pgacHIJKL*, the
409 Glc side chains are replaced with the GlcNAc side chains [50]. Interestingly, expression of
410 *gacHIJKL* in Δ*sccN* did not restore the resistance of the bacteria to PlyC (Fig. 5), indicating that
411 the GlcNAc side chains do not obstruct PlyC binding. Lastly, we analyzed PlyC-mediated lysis
412 of sacculi purified from the Δ*rgpG* mutant, which is deficient in SCC expression [50]. The RgpG
413 protein catalyzes the first step in SCC biosynthesis [51]. In comparison to Δ*sccN*, PlyC-induced
414 lysis of Δ*rgpG* was less pronounced (Fig. 5), indicating the importance of the pRha backbone of
415 SCC in PlyC activity and supporting the findings that the pRha backbone is a ligand contributing
416 to PlyC binding. These studies reveal that if the SCC is 'unmasked' *i.e.,* stripped of the Glc and
417 Glc-GroP side chains, it becomes a ligand for PlyCB and that *S. mutans* is PlyC susceptible if
418 SCC is replaced with GAC.
419

420 **Molecular Dynamics simulations identify novel binding pocket in PlyC**

421 Our biochemical investigations revealed that PlyCB interacts directly with the pRha backbone of
422 the GAC as shown in the cellular context of the native streptococcal cells, engineered *E. coli*
423 cells and *S. mutans* mutant strains. In contrast, traditional biochemical techniques such as size
424 exclusion chromatography or isothermal titration calorimetry could not detect the binding of
425 PlyCB when either the short or long pRha fragments were used (data not shown). These results
426 corroborate the previous studies on related proteins, showing that the binding between
427 endolysins to their respective isolated or purified cell wall ligands is challenging to characterize
428 [52, 53]. However, the CBD is a carbohydrate binding module, which often contains the
429 prominent binding sites to selectively coordinate the binding of linear polysaccharides (reviewed
430 in [54]). To identify the prominent binding sites for pRha, we investigated the previously reported
431 crystal structures of $PlyCB_{WT}$ and $PlyCB_{R66E}$ with the ligand site identification software SiteMap
432 [55]. The software identifies cavities on the molecular surface of a protein structure and provides
433 a 'druggability score', which indicates the likelihood that an identified site can bind a small
434 molecule. Interestingly, for both $PlyCB_{WT}$ and $PlyCB_{R66E}$ protein structures, no druggable sites
435 were identified (SF2). In the $PlyCB_{WT}$ structure, a small shallow cavity in proximity of R66 was
436 identified, but with a very poor druggability score (0.4). Shen *et al.*, had previously reported a
437 putative phosphate binding site in PlyCB [56], however, we concluded from our studies that no
438 pocket or cavity is large enough to accommodate the pRha structure. Protein crystal structures
439 represent a fixed conformation state that does not have to reflect the native fold in solution or in
440 the context of the respective ligands. Riley *et al.* reported previously a PlyCB SAXS in solution
441 structure [57] where a high degree of flexibility and movement of the PlyCB octameric ring was
442 revealed. We therefore conducted Molecular Dynamics (MD) simulations on the $PlyCB_{WT}$
443 structure (PDB 4F87) [13] to investigate how the protein structure changes over time. The
444 structure was simulated as a monomeric protein for 500 ns in the explicit solvent mode.
445 Strikingly, the $PlyCB_{WT}$ structure changed into an 'open' conformation, where Y28 rotates and

446 remains stable in a new conformation, generating a novel pocket (SF3). In the WT crystal
447 structure, R29 establishes a salt bridge with E36 in the same β-hairpin and has a repulsive
448 interaction with R66 on the α-helix. This repulsive effect results in a higher mobility of the
449 terminal part of the β-strand which allows the stabilisation of an open conformation of Y28
450 (SF3). The stabilisation of the open conformation of Y28 opens a cavity that is clearly visible on
451 the molecular surface of the WT structure and is identified by SiteMap as a druggable binding
452 site (score 0.8) (SF2).
453
454 It is well reported in the literature that a PlyC holoenzyme formed by PlyCA and the $PlyCB_{R66E}$
455 mutant protein is not able to lyse GAS [56]. Our biochemical studies have revealed that the
456 $PlyCB_{R66E}$ mutant does not bind pRha. We therefore conducted MD simulations also on the
457 reported $PlyCB_{R66E}$ crystal structure. In agreement with the $PlyCB_{WT}$ protein simulations, the
458 structure was stable. Contrary to the $PlyCB_{WT}$ protein, the rotation of Y28 was not observed and
459 subsequently, no cavity/pocket is formed (SF4). We inspected the conformation of the mutated
460 residues in $PlyCB_{R66E}$. The side chain of R66E forms a stable salt bridge with R29, increasing
461 the structural rigidity and preventing the opening of Y28 (SF4). Interestingly, the site controlled
462 by Y28 is not at the protein-protein interface, but within the monomeric structure, suggesting
463 that a ligand binding pocket exists within the monomeric protein and is not at the interface of two
464 neighboring monomers (SF2 1B, Fig. 6).
465
466 **PlyCB-rhamnose di- and tri-saccharide docking reveals potential interactions**
467 The MD simulations revealed a potential ligand binding site in $PlyCB_{WT}$ that is generated after
468 the gatekeeper Y28 rotated towards the α-helix. We conducted ligand-protein docking using a
469 Rha di- and tri-saccharide, with both possible linkage configurations. The Rha disaccharide and
470 trisaccharide with a non-reducing end α1,2-Rha (SF5) produced the congruent docking results,

471 which we further analyzed (Fig. 6, SF6). The Rha disaccharide with the non-reducing end (1->3)
472 linkage appears to be stabilized by four hydrogen bond interactions (SF7 A, B). The terminal
473 reducing end Rha is within the hydrogen bond distance to S17 and T12, whilst the α1,3-linked
474 non-reducing end Rha is able to interact with the carbonyl backbone of F10. The identical
475 interactions are observed for the docked trisaccharide (SF7 C, D). In addition, the non-reducing
476 end Rha of the trisaccharide also interacts with the side chain hydroxyl groups of S54 and Q49
477 (SF7 C, D). When we carefully inspected the structural context of the Rha trisaccharide with the
478 terminal α1,2-linked Rha moieties, we detected the adjacent pockets that could potentially bind
479 the GlcNAc side chain linked to these Rha moieties (SF8 A, B). It is beyond the scope of this
480 study to confirm that these pockets have the ability to bind the GAC β-GlcNAc sidechain or in
481 fact the Group C Carbohydrate (GCC) β-GalNAc-GalNAc disaccharide. However, this model is
482 consistent with PlyCB binding the unmodified pRha backbone and the backbone decorated with
483 the GAC or GCC side chains. The model also explains why the *S. mutans* SCC — with the α-2-
484 Glc substitution on the α1,3-linked Rha — is not a ligand for the PlyCB protein. The identified
485 pocket does not allow the binding of the SCC with the side chain in this configuration (SF8 A,
486 C).
487
488 **Polyrhamnose binding pocket suggests the PlyC catalytic mechanism**
489 We further investigated the structural context of this binding pocket, which is perpendicular to
490 the PlyCB monomer-monomer interface. We superposed the reported PlyCA structure that also
491 contains the GlyH and CHAP amidase domains (Fig 7). This led to the intriguing discovery that
492 this model would not only explain the specificity of the enzyme, but also the substrate
493 recognition by the CHAP amidase and GlyH domains. The proposed pRha binding pocket is
494 perpendicular to the GlyH and CHAP amidase domains, that bind the PG backbone and
495 crosslinked peptides. Similar to wall teichoic acids[58], the GAC and GCC are likely directly

496 linked via their reducing end sugars to *N*-acetylmuramic acid (MurNAc) of PG. We observed that
497 the reducing end sugar of the docked complex points towards the GlyH and CHAP amidase
498 domains. When we compare this structural alignment with the architectural arrangement of the
499 crosslinked PG decorated with the GAC, the model greatly assists our understanding of
500 PlyCAactivity: the CHAP amidase domain cleaves the PG peptide bond. This allows the PG to
501 open up and slide into the GlyH domain, which removes the PG GlcNAc-MurNAc from the
502 reducing end. Concurrently, the GAC attached to the PG binds to the octameric PlyCB domains.
503 We docked a PG tetrasacharide into the reported PlyCA GlyH domain (Fig. 7). This positions
504 the PG in 5-7Å, the distance that the terminal GAC sugar, GlcNAc, could occupy [23].
505

506 **Concluding remarks**
507
508 Strikingly, our PlyC molecular dynamics simulations revealed a previously unknown
509 conformational change that exposes a potential carbohydrate binding site. Our simulations
510 agree with the reported flexibility of the PlyCB structure in solution, as determined by SAXS
511 studies [57]. The reported crystal structure represents a locked state that appears to be the
512 most stable configuration in the crystallization conditions, in absence of any ligand. The side
513 chain of Y28 acts as gatekeeper and conformational changes allow opening of a cavity that is
514 likely capable of recognizing the compounds in the size of several sugar residues. These
515 structural changes are possible due to an intrinsic flexibility introduced by the repulsion between
516 the side chains of R29 (adjacent to Y28) and R66 (SF3). Moreover, we propose a structural
517 feature of the PlyCB protein that explains why only certain streptococci are susceptible to PlyC's
518 lytic activity. The pRha decorated with an α–linked side chain sugar is not compatible with the
519 PlyCB ligand binding site and therefore only those streptococci expressing pRha decorated with
520 β-linked substituents, such as GlcNAc and GlcNAc-GroP are susceptible. This could potentially
521 be exploited for diagnostic purposes or in the case of SCC and Group G Streptococci, opens up

522 the potential for novel therapeutic approaches. If SCC was treated by PlyC in combination with
523 an additional enzyme that removes the α–linked side chains in these streptococcal
524 carbohydrates, this would expose the pRha backbone and subsequently make these strains
525 susceptible. The identification of the pRha ligand site could also be further exploited by directed
526 evolution approaches to generate PlyCB protein variants that are capable to bind the
527 carbohydrates from, for example, SCC and Group G Streptococci. Since our proposed ligand
528 binding site is on the surface of each PlyCB monomer mutagenesis would most likely not impact
529 the multimerization interface of the PlyCB octameric ring.
530
531 Whilst much has been learned about the structure and function of PlyC in the past 20 years,
532 many questions remain, specifically with respect to its interaction with the PG. Considering the
533 average length of the cellular pRha is 7-10 kDa [25] and that our MD simulations shows an
534 individual PlyCB monomer can bind its target ligand, the α1,2-1,3-pRha with or without β-
535 configured GlcNAc/GalNAc-side chains, it is inviting to speculate that an element of avidity is
536 responsible for tight binding of the PlyCB octamer to the streptococcal surface. We have
537 envisioned a model in Fig. 7, although further proof is needed to substantiate this hypothesis.
538 Another question lies in the actions of the EADs relative to the PlyCB octamer. PlyC clearly has
539 a high turnover as demonstrated in multiple biochemical assays. However, it is unknown if
540 PlyCB “docks” to the surface and the flexibility of the holoenzyme allows the PlyC EADs to
541 cleave multiple bonds in a localized area weakening the overall superstructure of the PG.
542 Alternatively, the enzymatic turnover could be dictated by a balance of on and off rates of the
543 EADs and CBD monomers leading to widespread hydrolysis of the PG. Lastly, it is unknown
544 whether PlyC binds, cleaves, and releases the PG at random points on the streptococcal
545 surface or works its way down a single strand of PG in a processive manner. It is noteworthy
546 that cellulase enzymes, which cleave the β1,4 glycosidic linkages in cellulose, possess a

547 catalytic domain, a flexible linker, and a cellulose binding domain, analogous to the traditional
548 endolysins. It has been demonstrated that energy is stored in the flexible linker can adopt
549 compact and extended configurations that allows the cellulase to move in a “caterpillar-like”
550 motion down a chain of cellulose [59, 60]. Although PlyC does not contain an equivalent flexible
551 linker, the octameric nature of PlyCB invites the possibility that it may interact with the
552 successive pRha strands allowing PlyC to depolymerize the PG in a zipper-like fashion.
553
554 In conclusion, the α1,2-1,3-pRha is the definite, minimal carbohydrate substrate for the PlyCB
555 subunit. We validated this by comprehensive experiments, using pRha recombinantly produced
556 in *E. coli*, and the *S. mutans* variants of the Rha-based polysaccharides. Furthermore, the MD
557 simulations and subsequent docking studies revealed a potential binding site for Rha tri-
558 saccharides. Further studies are needed to detail the dynamics of the PlyC holoenzyme on the
559 streptococcal surface and the interdomain interactions. Nonetheless, the work described here
560 provides valuable insight into the molecular interactions that define a PlyC’s host specificity,
561 which can inform the future studies as well as engineering approaches.
562
563 **Data Availability Statement**
564 No mandated datasets are associated with the paper.
565
566
567
568
569
570
571
572

573 **Figure Legend**

574 Fig 1)

575 A) Symbolic drawings of the carbohydrate structures of GAS (GAC), polyrhamnose backbone
576 (pRha) in GAVS and M1_d*gacI*, GCS (GCC), GGS (GGC) and *S. mutans* (SCC). For simplicity,
577 the reported glycerol phosphate of occasionally present on the GAC and SCC side chains have
578 been omitted. Repeat units are marked with brackets. The pRha backbone with alternating (α1-
579 >2) and (α1->3) linkages, whilst the α1->2 Rha being decorated with a β1->3 side chain is a
580 commonality among all PlyC susceptible strains. B) PlyC lysis of streptococcal pathogens.
581 Group A and Group C Streptococci serotypes are susceptible to PlyC-mediated lysis. Group G
582 Streptococci show limited susceptibility and *S. mutans* is resistant to PlyC lysis. Three SDSE
583 isolates that produce the GAC instead of GGC (SDSE_*gac*) are susceptible to PlyC treatment.

584

585 Fig 2)

586 Precipitation studies of purified PlyCB and GAC reveal direct interaction of PlyCB with GAC. A)
587 The PlyCB concentration is kept constant whilst the GAC concentration is varied. Visible
588 precipitate forms at the higher concentrations. B) The precipitate level is measured
589 spectrophotometrically at 340 nm and compared to the mutant $PlyCB_{R66E}$, which does not bind
590 the GAC. C) Coomassie stained and D) densitometry analysis of PlyCB protein from the
591 supernatant fraction and aggregates (pellets). E, F) The same dose dependency is observed
592 when the PlyCB concentration is varied. Arrowhead depicts PlyCB protein at 8 kDa.

593

594 Fig 3)

595 Representation of immunoblot analysis of the cell lysate of *E. coli* expressing the SCC and GAC
596 pRha and carrying an empty control plasmid (-ve). A) Blot was incubated with PlyCB-Alexa
597 Fluor® 647 ($PlyCB_{WT}^{AF647}$). B) Probing the same samples with the GAC antibodies confirms the
598 presence of GAC in the bands. Molecular mass markers are given in kDa.

599

600 Fig 4)

601 PlyCB binding to *E. coli* cells were investigated by flow cytometry after labelling with
602 $PlyCB_{WT}^{AF647}$ and $PlyCB_{R66E}^{AF645}$ mutant proteins. Blue: -ve control cells without pRha. Red:
603 pRha producing *E. coli* cells. Representative histograms are shown. A) Left panel: unstained
604 cells. Right panel: The anti-GAC antibodies (GAC-FITC) were used as a positive control to label
605 the *E. coli* cells producing pRha. The antibodies do not bind to the *E. coli* cells carrying an
606 empty plasmid (-ve). B) Left panel: $PlyCB_{WT}^{AF647}$ binds to the *E. coli* cells producing pRha, but
607 not to the *E. coli* cells carrying an empty plasmid (-ve). Right panel: $PlyCB_{R66E}^{AF645}$ does not
608 binds to the *E. coli* cells producing pRha.

609

610 Fig 5)

611 The PlyC-mediated lysis of sacculi purified from *S. mutans* strains. The lysis was monitored
612 after 10, 20, 30, 40, 50 and 60 min as a decrease in OD_{600}. Results are presented as a fold
613 change in OD_{600} of the sacculi incubated with PlyC *vs.* the sacculi incubated without PlyC. Data
614 points and error bars represent mean values of four biological replicates and standard deviation,
615 respectively. P-values were determined by two-way ANOVA with Dunnett's multiple
616 comparisons test.

617

618 Fig 6)

619 Bottom view of the PlyCB protein structures in surface representation. The octameric PlyCB
620 structure with brown A, C, E, G and orange B, D, F, H monomers. A) WT (GH and CHAP
621 domain omitted, 4f87.pdb) B) WT after MD with docked tri-Rha. The MD simulations have
622 revealed a novel pocket that could accommodate the binding of short Rha-polysaccharides.

623

624 Fig 7)

625 A schematic model of the proposed PlyC binding to the streptococcal cell wall. A) PlyC in the
626 complex with docked PG tetra-saccharide in the GlyH domain (red) and pRha tri-saccharides in
627 PlyCB subunits. B) A schematic model showing PlyC binding to peptidoglycan and pRha.
628 Sugars are drawn to scale, with green triangles (Rha), blue square (GlcNAc) and beige square
629 (MurNAc). Proposed PlyC activity: The EAD cleaves the PG peptide to open up the PG
630 backbones that subsequently enter the GlyH domain (red) for PG cleavage.

631

632 **FUNDING**

633 The HCD laboratory is supported by Wellcome and Royal Society Grant 109357/Z/15/Z and the
634 University of Dundee Wellcome Trust Funds 105606/Z/14/Z and Tenovus Scotland Large
635 Research Grant [T17/17]. HK is supported by the National Institute of Standards and
636 Technology (NIST). VAF is supported by Rockefeller University laboratory funds. NK is
637 supported by NIH grants R01 DE028916 from the NIDCR and R01 AI143690 from the NIAID.

638

639 **ACKNOWLEDGEMENTS**

640 We thank the CDC Streptococcus Lab and the Active Bacterial Core surveillance program for
641 sharing isolates isolate 20170556 (stG6.0), 20171682 (stC74A.0), 20154376 (stG245.0),
642 20173686 (stG652.0), 20170560 and 20176966 (stG485.0). We also thank Ryan Heselpoth,
643 Yang Shen, and Sara Linden for reagents, technical advice, and helpful discussion.

644

645

646 **References**

647 1 Fernandes, S. and Sao-Jose, C. (2018) Enzymes and Mechanisms Employed by Tailed
648 Bacteriophages to Breach the Bacterial Cell Barriers. Viruses. **10**
649 2 Nelson, D., Loomis, L. and Fischetti, V. A. (2001) Prevention and elimination of upper
650 respiratory colonization of mice by group A streptococci by using a bacteriophage lytic enzyme.
651 Proc Natl Acad Sci U S A. **98**, 4107-4112

652 3 Dams, D. and Briers, Y. (2019) Enzybiotics: Enzyme-Based Antibacterials as
653 Therapeutics. Adv Exp Med Biol. **1148**, 233-253
654 4 Love, M. J., Bhandari, D., Dobson, R. C. J. and Billington, C. (2018) Potential for
655 Bacteriophage Endolysins to Supplement or Replace Antibiotics in Food Production and Clinical
656 Care. Antibiotics (Basel). **7**
657 5 Schmelcher, M. and Loessner, M. J. (2020) Bacteriophage endolysins - extending their
658 application to tissues and the bloodstream. Curr Opin Biotechnol. **68**, 51-59
659 6 Heselpoth, R. D., Swift, S. M., Linden, S. B., Mitchell, M. S. and Nelson, D. C. (2018)
660 Enzybiotics: endolysins and bacteriocins. In Bacteriophages - biology, technology, and therapy
661 (Harper, D., Abedon, S. T., Burrowes, B. and McConvill, M., eds.), Springer International
662 Publishing, Dordrecht, The Netherlands
663 7 Loessner, M. J., Kramer, K., Ebel, F. and Scherer, S. (2002) C-terminal domains of
664 Listeria monocytogenes bacteriophage murein hydrolases determine specific recognition and
665 high-affinity binding to bacterial cell wall carbohydrates. Molecular microbiology. **44**, 335-349
666 8 Mesnage, S., Dellarole, M., Baxter, N. J., Rouget, J. B., Dimitrov, J. D., Wang, N.,
667 Fujimoto, Y., Hounslow, A. M., Lacroix-Desmazes, S., Fukase, K., Foster, S. J. and Williamson,
668 M. P. (2014) Molecular basis for bacterial peptidoglycan recognition by LysM domains. Nat
669 Commun. **5**, 4269
670 9 Evans, A. C. (1934) *Streptococcus* bacteriphage: a study of four serological types.
671 Public Health Rep. **49**, 1386-1401
672 10 Krause, R. M. (1957) Studies on bacteriophages of hemolytic streptococci. I. Factors
673 influencing the interaction of phage and susceptible host cell. J Exp Med. **106**, 365-384
674 11 Maxted, W. R. (1957) The active agent in nascent phage lysis of streptococci. J Gen
675 Microbiol. **16**, 584-595
676 12 Nelson, D., Schuch, R., Chahales, P., Zhu, S. and Fischetti, V. A. (2006) PlyC: a
677 multimeric bacteriophage lysin. Proc Natl Acad Sci U S A. **103**, 10765-10770
678 13 McGowan, S., Buckle, A. M., Mitchell, M. S., Hoopes, J. T., Gallagher, D. T., Heselpoth,
679 R. D., Shen, Y., Reboul, C. F., Law, R. H., Fischetti, V. A., Whisstock, J. C. and Nelson, D. C.
680 (2012) X-ray crystal structure of the streptococcal specific phage lysin PlyC. Proc Natl Acad Sci
681 U S A. **109**, 12752-12757
682 14 Lancefield, R. C. (1933) A Serological Differentiation of Human and Other Groups of
683 Hemolytic Streptococci. J Exp Med. **57**, 571-595
684 15 Vandamme, P., Pot, B., Falsen, E., Kersters, K. and Devriese, L. A. (1996) Taxonomic
685 study of lancefield streptococcal groups C, G, and L (Streptococcus dysgalactiae) and proposal
686 of S. dysgalactiae subsp. equisimilis subsp. nov. Int J Syst Bacteriol. **46**, 774-781
687 16 Coligan, J. E., Kindt, T. J. and Krause, R. M. (1978) Structure of the streptococcal
688 groups A, A-variant and C carbohydrates. Immunochemistry. **15**, 755-760
689 17 Pritchard D G, G. R. L., Michlek S M, McGhee J R. . (1986) Biochemical aspects of
690 serotype carbohydrate antigens of Streptococcus mutans. In: Hamada S, Michalek S M, Kiyono
691 H, Menaker L, McGhee J R, editors. Molecular microbiology and immunology of Streptococcus
692 mutans. Amsterdam, The Netherlands: . Elsevier Science Publishers; , pp. 39–49.
693 18 Coligan, J. E., Schnute, W. C., Jr. and Kindt, T. J. (1975) Immunochemical and chemical
694 studies on streptococcal group-specific carbohydrates. J Immunol. **114**, 1654-1658
695 19 Huang, D. H., Rama Krishna, N. and Pritchard, D. G. (1986) Characterization of the
696 group A streptococcal polysaccharide by two-dimensional ^{1}H-nuclear-magnetic-resonance
697 spectroscopy. Carbohydrate research. **155**, 193-199
698 20 Neiwert, O., Holst, O. and Duda, K. A. (2014) Structural investigation of rhamnose-rich
699 polysaccharides from Streptococcus dysgalactiae bovine mastitis isolate. Carbohydr Res. **389**,
700 192-195
701 21 Edgar, R. J., van Hensbergen, V. P., Ruda, A., Turner, A. G., Deng, P., Le Breton, Y.,
702 El-Sayed, N. M., Belew, A. T., McIver, K. S., McEwan, A. G., Morris, A. J., Lambeau, G.,

703 Walker, M. J., Rush, J. S., Korotkov, K. V., Widmalm, G., van Sorge, N. M. and Korotkova, N.
704 (2019) Discovery of glycerol phosphate modification on streptococcal rhamnose
705 polysaccharides. Nature chemical biology. **15**, 463-471
706 22 van der Beek, S. L., Zorzoli, A., Canak, E., Chapman, R. N., Lucas, K., Meyer, B. H.,
707 Evangelopoulos, D., de Carvalho, L. P. S., Boons, G. J., Dorfmueller, H. C. and van Sorge, N.
708 M. (2019) Streptococcal dTDP-L-rhamnose biosynthesis enzymes: functional characterization
709 and lead compound identification. Molecular microbiology. **111**, 951-964
710 23 Zorzoli, A., Meyer, B. H., Adair, E., Torgov, V. I., Veselovsky, V. V., Danilov, L. L., Uhrin,
711 D. and Dorfmueller, H. C. (2019) Group A, B, C, and G Streptococcus Lancefield antigen
712 biosynthesis is initiated by a conserved alpha-d-GlcNAc-beta-1,4-l-rhamnosyltransferase. J Biol
713 Chem. **294**, 15237-15256
714 24 van der Beek, S. L., Le Breton, Y., Ferenbach, A. T., Chapman, R. N., van Aalten, D. M.,
715 Navratilova, I., Boons, G. J., McIver, K. S., van Sorge, N. M. and Dorfmueller, H. C. (2015)
716 GacA is essential for Group A Streptococcus and defines a new class of monomeric dTDP-4-
717 dehydrorhamnose reductases (RmlD). Molecular microbiology. **98**, 946-962
718 25 Rush, J. S., Edgar, R. J., Deng, P., Chen, J., Zhu, H., van Sorge, N. M., Morris, A. J.,
719 Korotkov, K. V. and Korotkova, N. (2017) The molecular mechanism of N-acetylglucosamine
720 side-chain attachment to the Lancefield group A carbohydrate in Streptococcus pyogenes. J
721 Biol Chem. **292**, 19441-19457
722 26 Lood, R., Raz, A., Molina, H., Euler, C. W. and Fischetti, V. A. (2014) A highly active and
723 negatively charged Streptococcus pyogenes lysin with a rare D-alanyl-L-alanine endopeptidase
724 activity protects mice against streptococcal bacteremia. Antimicrob Agents Chemother. **58**,
725 3073-3084
726 27 Gera, K. and McIver, K. S. (2013) Laboratory growth and maintenance of Streptococcus
727 pyogenes (the Group A Streptococcus, GAS). Curr Protoc Microbiol. **30**, 9D 2 1-9D 2 13
728 28 Shibata, Y., Yamashita, Y., Ozaki, K., Nakano, Y. and Koga, T. (2002) Expression and
729 characterization of streptococcal rgp genes required for rhamnan synthesis in Escherichia coli.
730 Infect Immun. **70**, 2891-2898
731 29 DuBois, M., Gilles, K. A., Hamilton, J. K., Rebers, P. A. and Smith, F. (1956) Colorimetric
732 method for determination of sugars and related substances. Anal. Chem. **28**, 350-356
733 30 Heselpoth, R. D., Yin, Y., Moult, J. and Nelson, D. C. (2015) Increasing the stability of
734 the bacteriophage endolysin PlyC using rationale-based FoldX computational modeling. Protein
735 Eng Des Sel. **28**, 85-92
736 31 Case DA, e. a. (2016) AMBER2016. University of California, San Francisco
737
738 32 Maier, J. A., Martinez, C., Kasavajhala, K., Wickstrom, L., Hauser, K. E. and Simmerling,
739 C. (2015) ff14SB: Improving the Accuracy of Protein Side Chain and Backbone Parameters
740 from ff99SB. J Chem Theory Comput. **11**, 3696-3713
741 33 Darden, T. A. and Pedersen, L. G. (1993) Molecular modeling: an experimental tool.
742 Environ Health Perspect. **101**, 410-412
743 34 Jean-Paul Ryckaert, G. C., Herman J.C Berendsen. (1977) Numerical integration of the
744 cartesian equations of motion of a system with constraints: molecular dynamics of n-alkanes.
745 Journal of Computational Physics. **23**, 327-341
746 35 DeLano, W. L. (2002) The PyMOL Molecular Graphics System. Delano Scientific, San
747 Carlos.
748 36 William Humphrey, A. D., Klaus Schulten. (1996) VMD: Visual molecular dynamics.
749 Journal of Molecular Graphics. **14**, 33-38
750 37 2021-1:, S. R. (2021) LigPrep Schrödinger, LLC, New York, NY
751 38 M., M. (1952) The lysis of group A hemolytic streptococci by extracellular enzymes of
752 Streptomyces albus. II. Nature of the cellular substrate attacked by the lytic enzymes. . J Exp
753 Med. . **96**, 569–580

754 39 Davies, M. R., McIntyre, L., Mutreja, A., Lacey, J. A., Lees, J. A., Towers, R. J.,
755 Duchene, S., Smeesters, P. R., Frost, H. R., Price, D. J., Holden, M. T. G., David, S., Giffard, P.
756 M., Worthing, K. A., Seale, A. C., Berkley, J. A., Harris, S. R., Rivera-Hernandez, T., Berking,
757 O., Cork, A. J., Torres, R., Lithgow, T., Strugnell, R. A., Bergmann, R., Nitsche-Schmitz, P.,
758 Chhatwal, G. S., Bentley, S. D., Fraser, J. D., Moreland, N. J., Carapetis, J. R., Steer, A. C.,
759 Parkhill, J., Saul, A., Williamson, D. A., Currie, B. J., Tong, S. Y. C., Dougan, G. and Walker, M.
760 J. (2019) Author Correction: Atlas of group A streptococcal vaccine candidates compiled using
761 large-scale comparative genomics. Nat Genet. **51**, 1295
762 40 Brandt, C. M., Haase, G., Schnitzler, N., Zbinden, R. and Lutticken, R. (1999)
763 Characterization of blood culture isolates of Streptococcus dysgalactiae subsp. equisimilis
764 possessing Lancefield's group A antigen. J Clin Microbiol. **37**, 4194-4197
765 41 Chochua, S., Metcalf, B. J., Li, Z., Rivers, J., Mathis, S., Jackson, D., Gertz, R. E., Jr.,
766 Srinivasan, V., Lynfield, R., Van Beneden, C., McGee, L. and Beall, B. (2017) Population and
767 Whole Genome Sequence Based Characterization of Invasive Group A Streptococci Recovered
768 in the United States during 2015. mBio. **8**
769 42 McMillan, D. J., Vu, T., Bramhachari, P. V., Kaul, S. Y., Bouvet, A., Shaila, M. S.,
770 Karmarkar, M. G. and Sriprakash, K. S. (2010) Molecular markers for discriminating
771 Streptococcus pyogenes and S. dysgalactiae subspecies equisimilis. Eur J Clin Microbiol Infect
772 Dis. **29**, 585-589
773 43 Lynskey, N. N., Jauneikaite, E., Li, H. K., Zhi, X., Turner, C. E., Mosavie, M., Pearson,
774 M., Asai, M., Lobkowicz, L., Chow, J. Y., Parkhill, J., Lamagni, T., Chalker, V. J. and
775 Sriskandan, S. (2019) Emergence of dominant toxigenic M1T1 Streptococcus pyogenes clone
776 during increased scarlet fever activity in England: a population-based molecular epidemiological
777 study. Lancet Infect Dis. **19**, 1209-1218
778 44 Pritchard, D. G., Rener, B. P., Furner, R. L., Huang, D. H. and Krishna, N. R. (1988)
779 Structure of the group G streptococcal polysaccharide. Carbohydr Res. **173**, 255-262
780 45 Mirica, K. A., Lockett, M. R., Snyder, P. W., Shapiro, N. D., Mack, E. T., Nam, S. and
781 Whitesides, G. M. (2012) Selective precipitation and purification of monovalent proteins using
782 oligovalent ligands and ammonium sulfate. Bioconjug Chem. **23**, 293-299
783 46 Sato, T., Mattison, K. W., Dubin, P. L., Kamachi, M. and Morishima, Y. (1998) Effect of
784 protein aggregation on the binding of lysozyme to pyrene-labeled polyanions. Langmuir. **14**,
785 5430-5437
786 47 Wilcken, R., Wang, G., Boeckler, F. M. and Fersht, A. R. (2012) Kinetic mechanism of
787 p53 oncogenic mutant aggregation and its inhibition. Proc Natl Acad Sci U S A. **109**, 13584-
788 13589
789 48 Michon, F., Moore, S. L., Kim, J., Blake, M. S., Auzanneau, F. I., Johnston, B. D.,
790 Johnson, M. A. and Pinto, B. M. (2005) Doubly branched hexasaccharide epitope on the cell
791 wall polysaccharide of group A streptococci recognized by human and rabbit antisera. Infect
792 Immun. **73**, 6383-6389
793 49 van Sorge, N. M., Cole, J. N., Kuipers, K., Henningham, A., Aziz, R. K., Kasirer-Friede,
794 A., Lin, L., Berends, E. T. M., Davies, M. R., Dougan, G., Zhang, F., Dahesh, S., Shaw, L., Gin,
795 J., Cunningham, M., Merriman, J. A., Hutter, J., Lepenies, B., Rooijakkers, S. H. M., Malley, R.,
796 Walker, M. J., Shattil, S. J., Schlievert, P. M., Choudhury, B. and Nizet, V. (2014) The classical
797 lancefield antigen of group a Streptococcus is a virulence determinant with implications for
798 vaccine design. Cell Host Microbe. **15**, 729-740
799 50 Svetlana Zamakhaeva, C. T. C., Jeffrey S. Rush, Sowmya Ajay Castro, Alexander E.
800 Yarawsky, Andrew B. Herr, Nina M. van Sorge, Helge C. Dorfmueller, Gregory I. Frolenkov,
801 Konstantin V. Korotkov, Natalia Korotkova. (2020) Modification of cell wall polysaccharide
802 spatially controls cell division in Streptococcus mutans. bioRxiv
803 51 De, A., Liao, S., Bitoun, J. P., Roth, R., Beatty, W. L., Wu, H. and Wen, Z. T. (2017)
804 Deficiency of RgpG causes major defects in cell division and biofilm formation, and deficiency of

LytR-CpsA-Psr family proteins leads to accumulation of cell wall antigens in culture medium by *Streptococcus mutans*. Appl Environ Microbiol. **83**

52 Ganguly, J., Low, L. Y., Kamal, N., Saile, E., Forsberg, L. S., Gutierrez-Sanchez, G., Hoffmaster, A. R., Liddington, R., Quinn, C. P., Carlson, R. W. and Kannenberg, E. L. (2013) The secondary cell wall polysaccharide of Bacillus anthracis provides the specific binding ligand for the C-terminal cell wall-binding domain of two phage endolysins, PlyL and PlyG. Glycobiology. **23**, 820-832

53 Shen, Y., Kalograiaki, I., Prunotto, A., Dunne, M., Boulos, S., Taylor, N. M. I., Sumrall, E. T., Eugster, M. R., Martin, R., Julian-Rodero, A., Gerber, B., Leiman, P. G., Menendez, M., Dal Peraro, M., Canada, F. J. and Loessner, M. J. (2021) Structural basis for recognition of bacterial cell wall teichoic acid by pseudo-symmetric SH3b-like repeats of a viral peptidoglycan hydrolase. Chemical Science. **12**, 576-589

54 Shoseyov, O., Shani, Z. and Levy, I. (2006) Carbohydrate binding modules: biochemical properties and novel applications. Microbiol Mol Biol Rev. **70**, 283-295

55 Halgren, T. (2007) New method for fast and accurate binding-site identification and analysis. Chem Biol Drug Des. **69**, 146-148

56 Shen, Y., Barros, M., Vennemann, T., Gallagher, D. T., Yin, Y., Linden, S. B., Heselpoth, R. D., Spencer, D. J., Donovan, D. M., Moult, J., Fischetti, V. A., Heinrich, F., Losche, M. and Nelson, D. C. (2016) A bacteriophage endolysin that eliminates intracellular streptococci. eLife. **5**

57 Riley, B. T., Broendum, S. S., Reboul, C. F., Cowieson, N. P., Costa, M. G., Kass, I., Jackson, C., Perahia, D., Buckle, A. M. and McGowan, S. (2015) Dynamic Motion and Communication in the Streptococcal C1 Phage Lysin, PlyC. PLoS One. **10**, e0140219

58 Brown, S., Santa Maria, J. P., Jr. and Walker, S. (2013) Wall teichoic acids of gram-positive bacteria. Annu Rev Microbiol. **67**, 313-336

59 Rabinovich, M. L., Melnick, M. S. and Bolobova, A. V. (2002) The structure and mechanism of action of cellulolytic enzymes. Biochemistry (Mosc). **67**, 850-871

60 McCabe, C., Zhao, X., Adney, W. S., Himmel, M. E. (2010) Energy Storage in Cellulase Linker Peptides? Computational Modeling in Lignocellulosic Biofuel Production. **1052**, 119-134

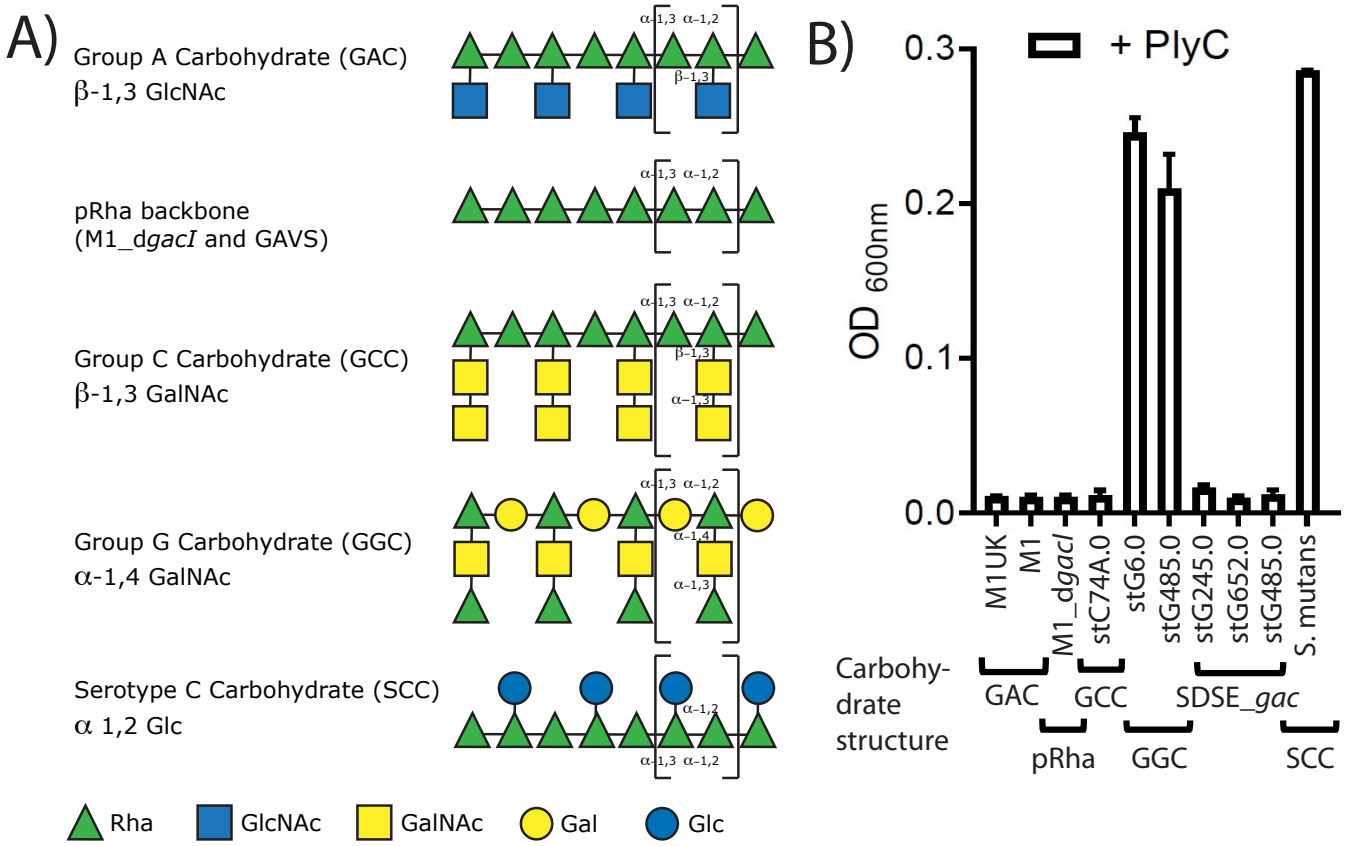

Fig 1)
A) Symbolic drawings of the carbohydrate structures of GAS (GAC), polyrhamnose backbone (pRha) in GAVS and M1_d*gacI*, GCS (GCC), GGS (GGC) and S. mutans (SCC). For simplicity, the reported glycerol phosphate of occasionally present on the GAC and SCC side chains have been omitted. Repeat units are marked with brackets. The pRha backbone with alternating (α1->2) and (α1->3) linkages, whilst the α1->2 rhamnose being decorated with a β1->3 side chain is a commonality among all PlyC susceptible strains. B) PlyC lysis of streptococcal pathogens. Group A and Group C Streptococci serotypes are susceptible to PlyC-mediated lysis. Group G Streptococci show limited susceptibility and S. mutans is resistant to PlyC lysis. Three SDSE isolates that produce the GAC instead of GGC (SDSE_*gac*) are susceptible to PlyC treatment.

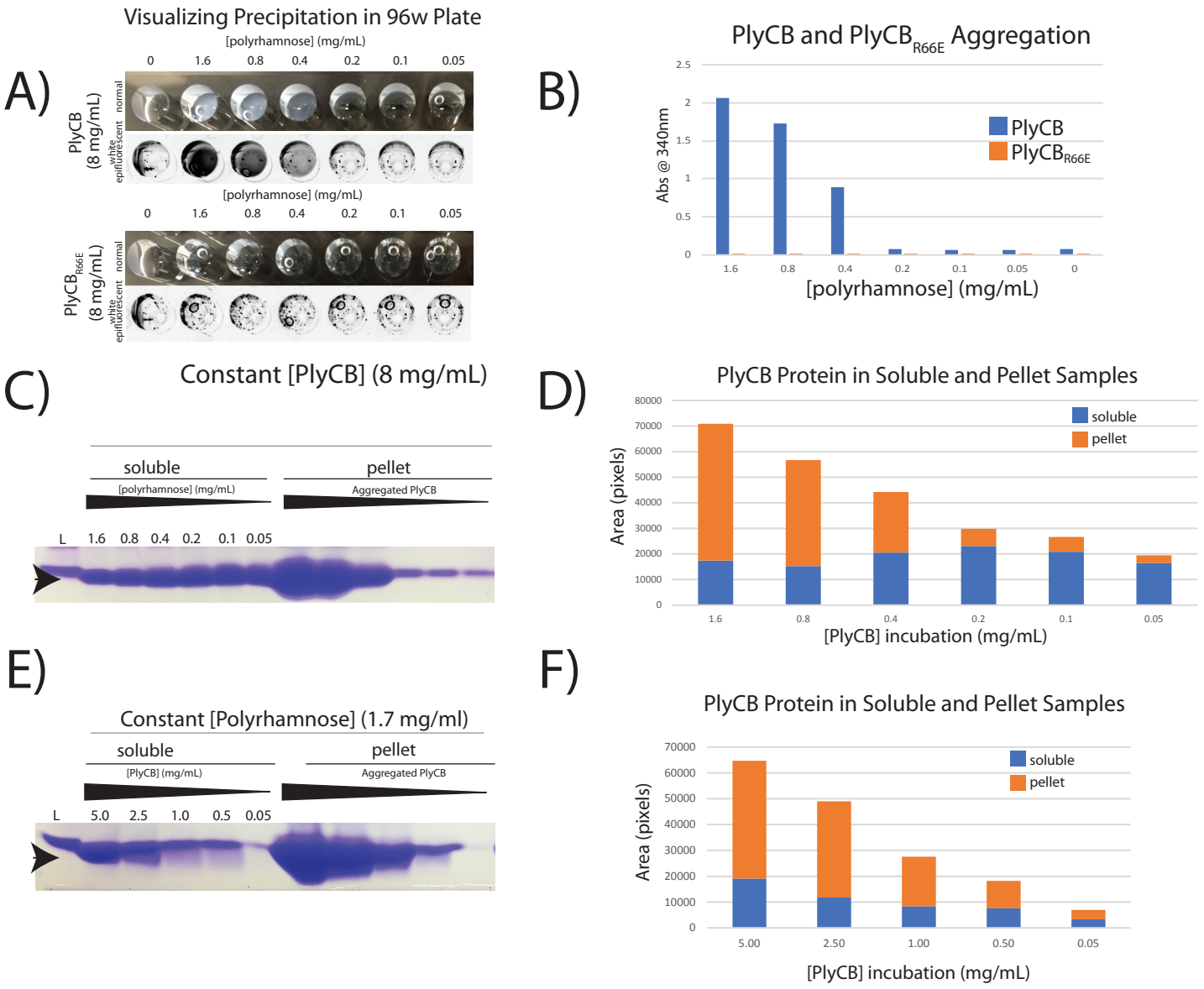

Fig 2)
Precipitation studies of purified PlyCB and GAC reveal direct interaction of PlyCB with GAC. A) The PlyCB concentration is kept constant whilst the GAC concentration is varied. Visible precipitate forms at the higher concentrations. B) The precipitate level is measured spectrophotometrically at 340 nm and compared to the mutant PlyCB_R66E, which does not bind the GAC. C) Coomassie stained and D) densitometry analysis of PlyCB protein from the supernatant fraction and aggregates (pellets). E, F) The same dose dependency is observed when the PlyCB concentration is varied. Arrowhead depicts PlyCB protein (8 kDa).

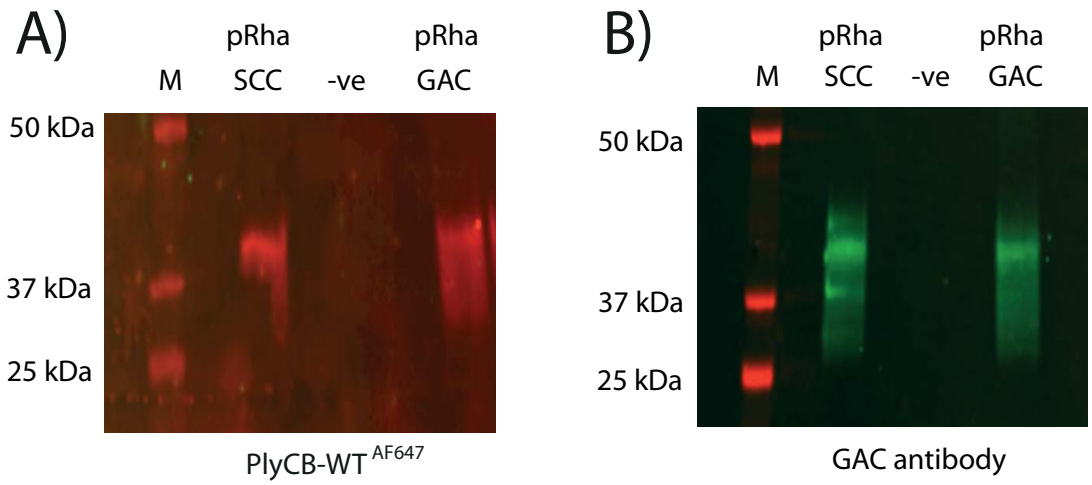

Fig 3)
Representation of immunoblot analysis of the cell lysate of E. coli expressing the SCC and GAC pRha and carrying an empty control plasmid (-ve). A) Blot was incubated with PlyCB-Alexa Fluor® 647 (PlyCB-WT-AF647). B) Probing the same samples with the GAC antibodies confirms the presence of GAC in the bands. Molecular mass markers are given in kDa.

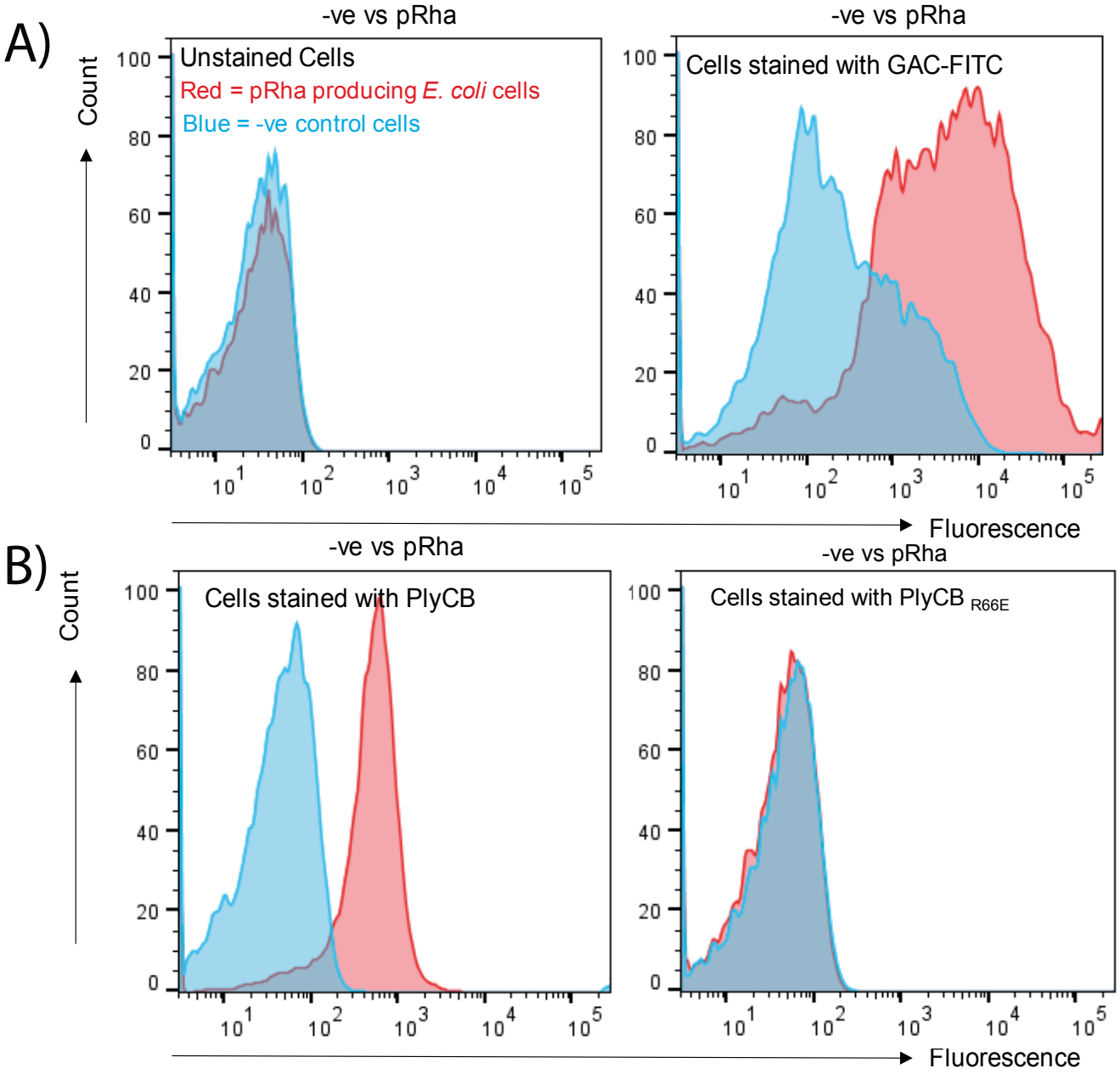

Fig 4)

PlyCB binding to *E. coli* cells were investigated by flow cytometry after labelling with $PlyCB_{WT}^{AF647}$ and $PlyCB_{R66E}^{AF645}$ mutant proteins. Blue: -ve control cells without pRha. Red: pRha producing *E. coli* cells. Representative histograms are shown. A) Left panel: unstained cells. Right panel: The anti-GAC antibodies (GAC-FITC) were used as a positive control to label the *E. coli* cells producing pRha. The antibodies do not bind to the E. coli cells carrying an empty plasmid (-ve). B) Left panel: $PlyCB_{WT}^{AF647}$ binds to the *E. coli* cells producing pRha, but not to the *E. coli* cells carrying an empty plasmid (-ve). Right panel: $PlyCB_{R66E}^{AF645}$ does not binds to the *E. coli* cells producing pRha.

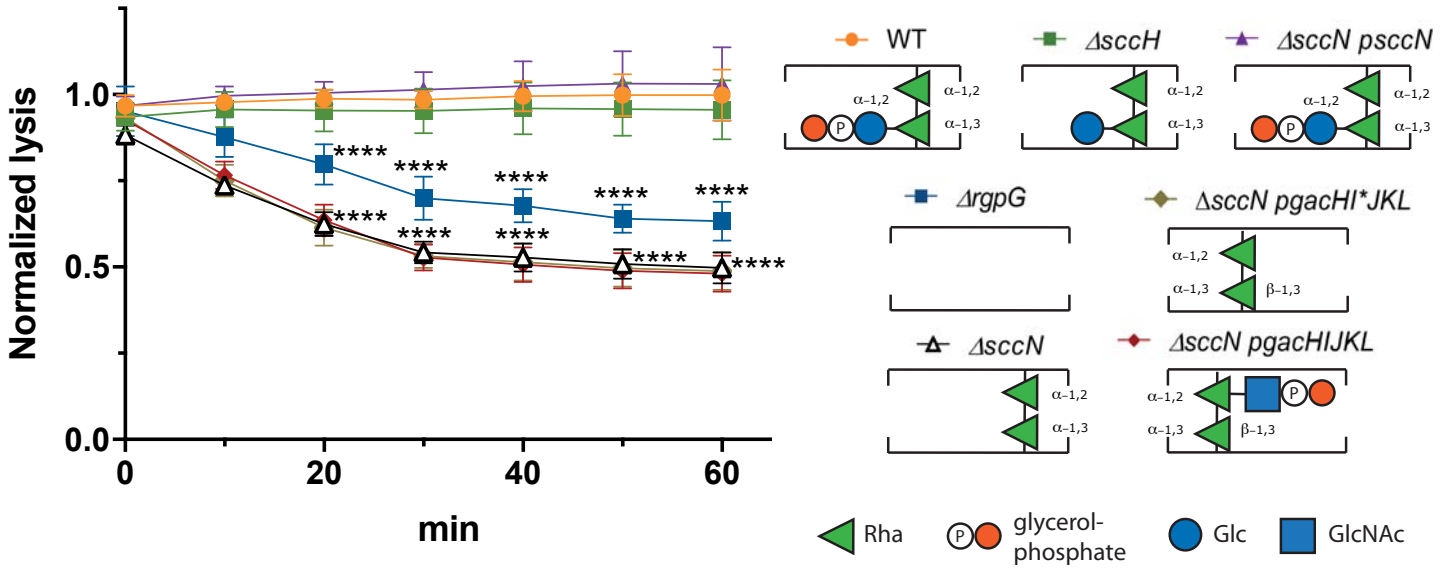

Fig 5)
The PlyC-mediated lysis of sacculi purified from *S. mutans* strains. The lysis was monitored after 10, 20, 30, 40, 50 and 60 min as a decrease in OD_{600}. Results are presented as a fold change in OD_{600} of the sacculi incubated with PlyC *vs.* the sacculi incubated without PlyC. Data points and error bars represent mean values of four biological replicates and standard deviation, respectively. P-values were determined by two-way ANOVA with Dunnett's multiple comparisons test.

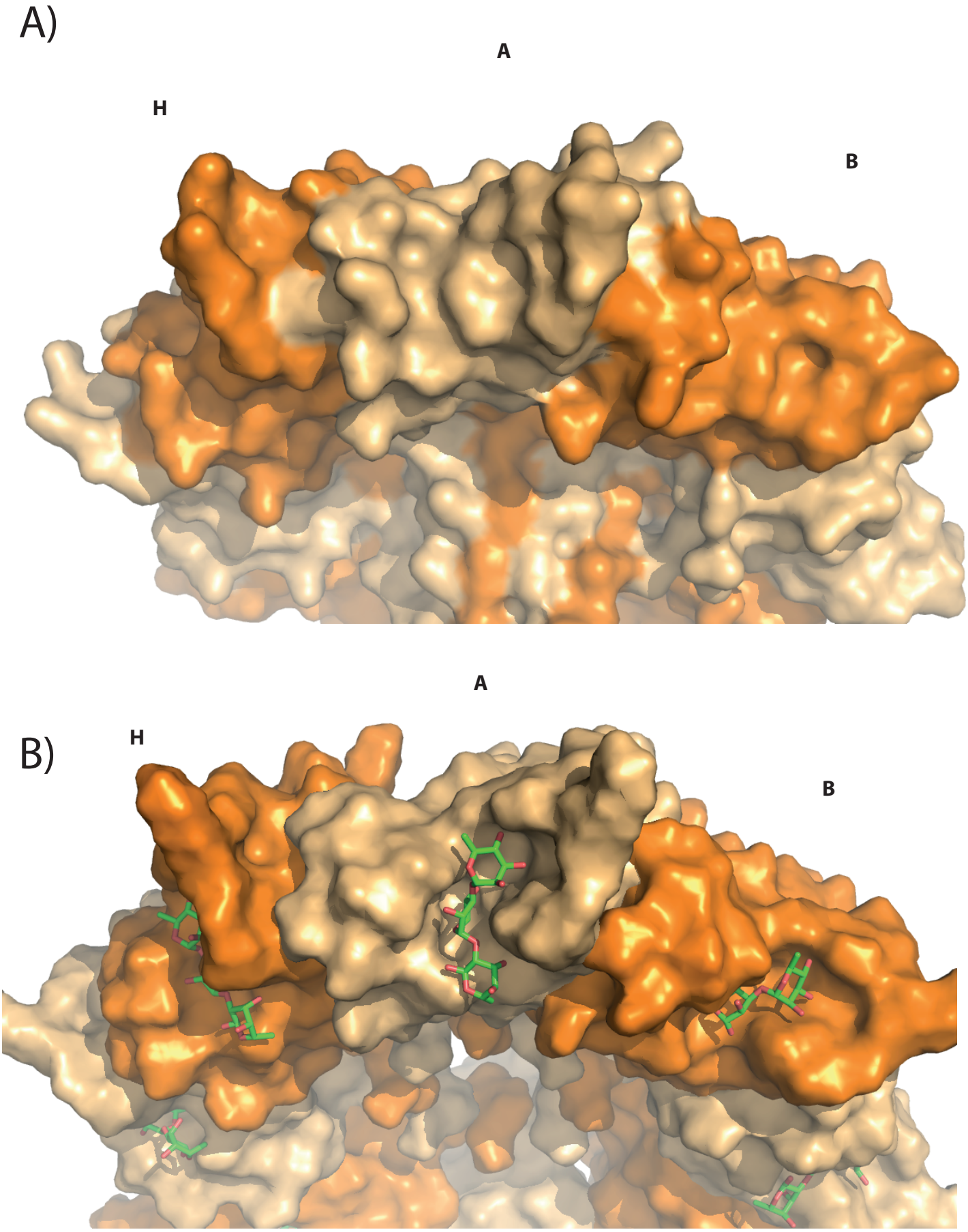

Fig 6)
Bottom view of the PlyCB protein structures in surface representation. The octameric PlyCB structure with brown A, C, E, G and orange B, D, F, H monomers. A) WT (GH and CHAP domain omitted, 4f87.pdb) B) WT after MD with docked tri-rhamnose. The MD simulations have revealed a novel pocket that could accommodate the binding of short rhamnose-polysaccharides.

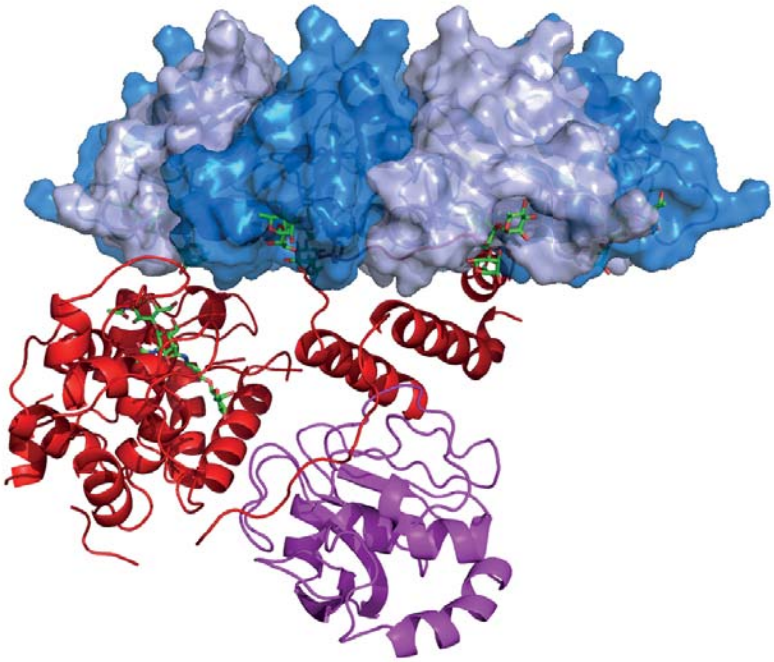

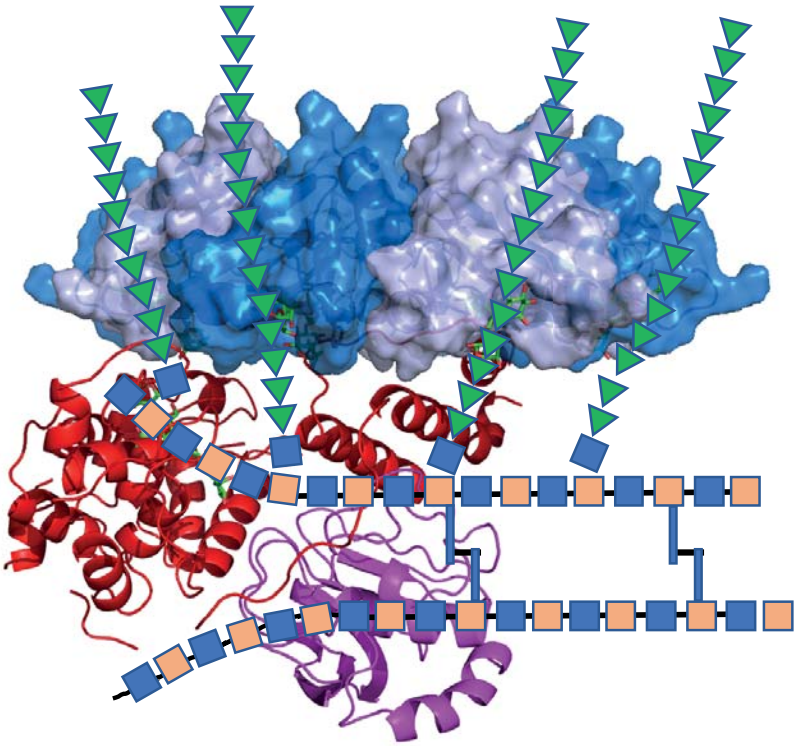

Fig 7)
A schematic model of the proposed PlyC binding to the streptococcal cell wall. A) PlyC in the complex with docked PG tetra-saccharide in the GH domain (red) and polyrhamnose tri-saccharides in PlyCB subunits. B) A schematic model showing PlyC binding to peptidoglycan and polyrhamnose. Sugars are drawn to scale, with green triangles (rhamnose), blue square (GlcNAc) and beige square (MurNAc). Proposed PlyC activity: The EAD cleaves the PG peptide to open up the PG backbones that subsequently enter the GH domain (red) for PG cleavage.